

A Framework to Segment Cellular Ultrastructure from 3D Electron Microscopy Images of Human Biopsies

Archana Machireddy¹, Guillaume Thibault^{2,5}, Cecilia E. Bueno^{2,5}, Hannah R. Smith², Jessica L. Riesterer^{2,3,5}, Joe W. Gray^{2,5} and Xubo Song^{1,2,4}

¹. Computer Science and Electrical Engineering, Oregon Health and Science University, Portland, OR, USA.

². Department of Biomedical Engineering, Oregon Health & Science University, Portland, OR, USA.

³. Multiscale Microscopy Core, Oregon Health & Science University, Portland, OR, USA.

⁴. Department of Medical Informatics and Clinical Epidemiology at Oregon Health and Science University, Portland, OR, USA.

⁵. Knight Cancer Institute, Oregon Health & Science University, Portland, OR, USA.

* Corresponding author: machired@ohsu.edu

A deeper understanding of the cellular and subcellular organization of tumor cells and their interactions with the tumor microenvironment will shed light on how cancer evolves and guide effective therapy choices. Electron microscopy (EM) images can provide detailed view of the cellular ultrastructure and are being generated at an ever-increasing rate. However, the bottleneck in their analysis is the delineation of the cellular structures to enable interpretable rendering. We have mitigated this limitation by using deep learning to segment cells and subcellular ultrastructure.

We segmented the cells, nuclei, nucleoli, mitochondria, endosomes and lysosomes in 3D focused ion beam-scanning electron microscopy (FIB-SEM) images of three tumor biopsies obtained from two patients with metastatic breast (Bx1, Bx2) and pancreatic (PDAC) cancers, respectively, and a microspheroid prepared using a breast cancer cell line (MCF7). All tissues were imaged with an isotropic resolution of 4 nm. The targeted intracellular organelles exhibited distinct appearances from the surrounding ultrastructure, allowing training of machine learning methods for semi-automated segmentation. ResUNet - a deep-learning architecture for image segmentation (Figure 2A) - trained with sparse manual labels resulted in accurate segmentation of nuclei, nucleoli and mitochondria with best Dice scores of 0.99, 0.98 and 0.86 respectively. In addition to the segmentation of the nucleoli, the method enabled visualization of the fenestrations within (Figure 2E). Segmentation performances of endosomes and lysosomes were evaluated qualitatively (Figure 1) as they were labelled only on a few slices that were used to train the ResUNet model.

Unlike organelle segmentation [1, 2, 3], the segmentation of cells in FIB-SEM images of non-neural tissues has not been widely explored [4]. It is a complex task due to the lack of clear boundaries separating cancer cells. Therefore, methods designed for the widely studied neural cells that use cell boundaries as the strongest cue for delineation cannot be directly applied for cancer cell segmentation [1, 5]. The convoluted and intertwined nature of cancer cells and the presence of filopodia-like protrusions make it even more challenging. We chose a multi-pronged approach combining segmentation, propagation and tracking strategies for cell segmentation. ResUNet was employed to segment the intra-cellular space and optical flow [6] was used to propagate the cell boundaries from the nearest ground truth image to facilitate separation of individual cells. Finally, the filopodia-like protrusions were tracked to the main cells by calculating the intersection over union measure for all regions detected in consecutive images and connecting regions with maximum overlap. The proposed

cell segmentation methodology resulted in a best Dice score of 0.99. Figures 2C and 2D show the volume renderings of the FIB-SEM image stack and the predicted segmentation masks of cells and organelles for the PDAC dataset. Figure 2F shows the performance gain of the proposed multi-pronged cell segmentation framework over standalone segmentation or propagation methods per cell in Bx1 dataset. Figure 1 shows 2D image slices overlaid with ground truth and predicted segmentations for all datasets. It also shows the volume occupied by the predicted organelles per cell in each dataset.

Segmentation of cells and their organelles allowed us to characterize biologically relevant features such as their morphology and texture. The morphological measures were designed to capture the size and shape (figure 2G and 2H), while the texture features captured the spatial distribution of intensity patterns. These features are capable of capturing the differences between the samples, and can be potentially linked to biologically or clinically relevant variables such as patient drug response in downstream analysis. The proposed segmentation of EM images enabling interpretative rendering and quantitative analysis, fills the gap that has prevented modern EM imaging from being used routinely for research and clinical practices [7].

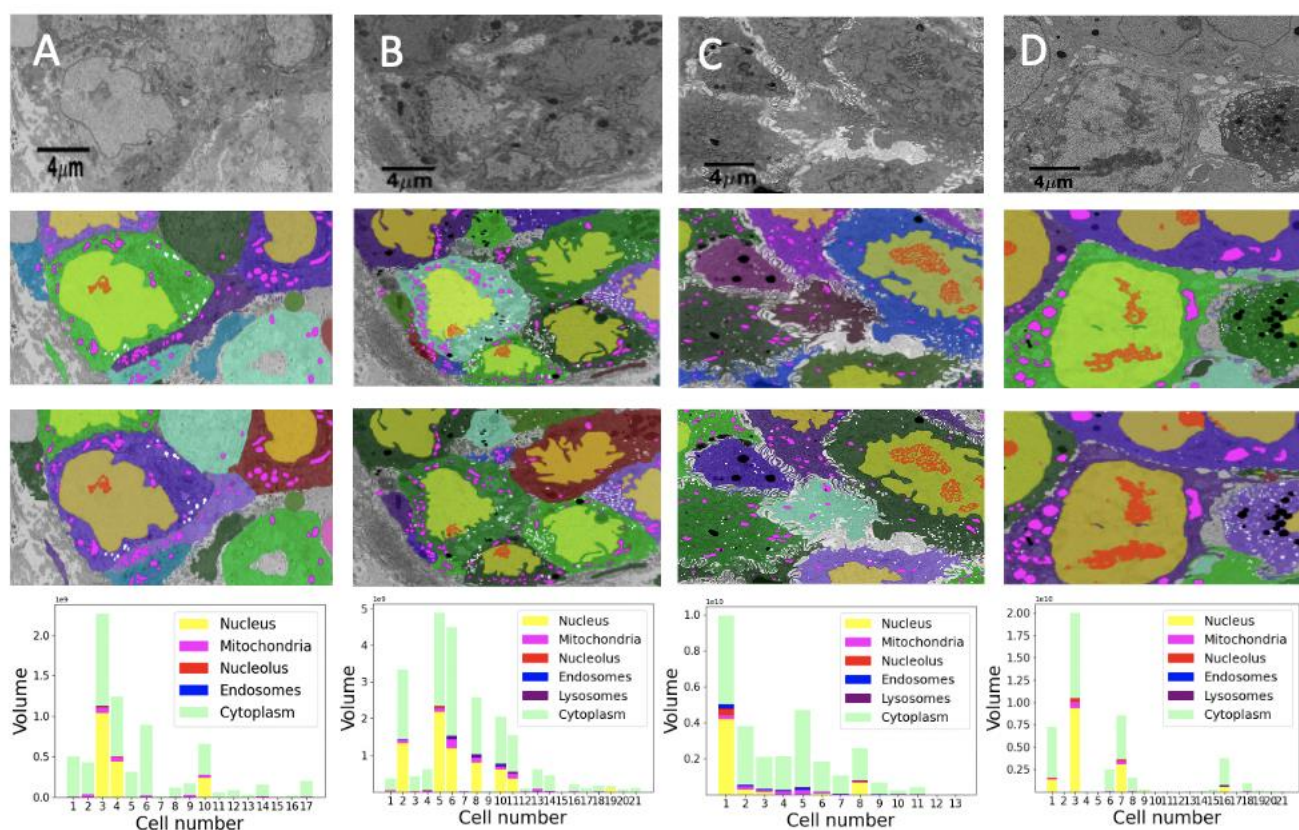


Figure 1. Qualitative results showing input images (first row) overlaid with nuclei (yellow), nucleoli (red), mitochondria (pink), endosomes (white), lysosomes (black) and cell segmentation (random colors) on ground truth masks (second row) and predicted segmentation masks (third row) for (A) Bx1 (B) Bx2, (C) PDAC, and (D) MCF7 datasets. The fourth row shows the volume occupied by the predicted organelles for each cell in each dataset.

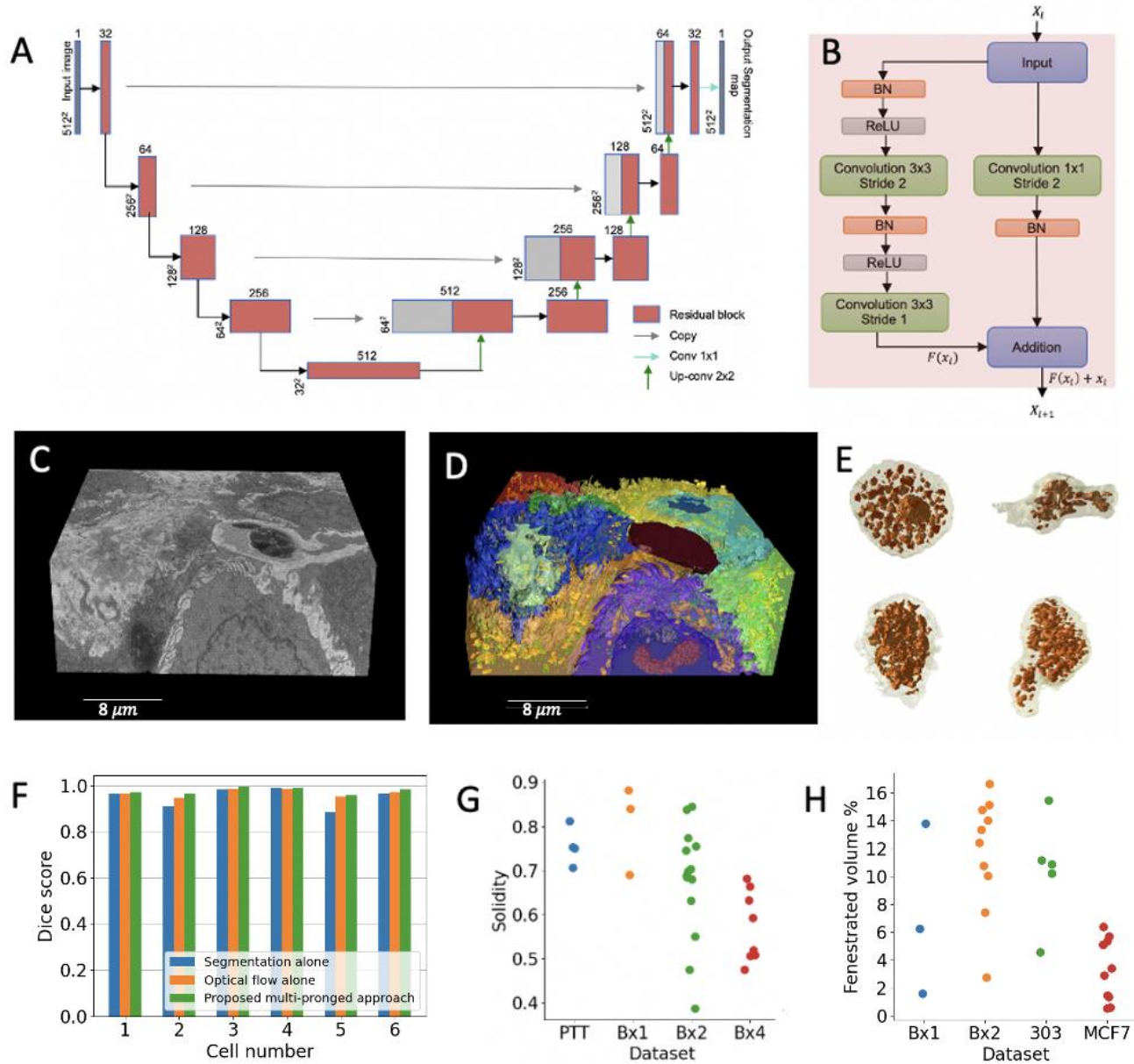


Figure 2. (A) ResUNet architecture, input size is written on the side of each box. The number of feature maps in each residual layer is written on top of each box. (B) Residual block used in ResUNet, BN stands for batch normalization and ReLU stands for rectified linear unit. X_l and X_{l+1} are the input and output features for the residual layer l , and F represents the residual function (C) Volume renderings showing the FIB-SEM image stack and (D) the predicted segmentation masks of cells and organelles for the PDAC dataset, (E) Volume renderings of the fenestrations in nucleoli from different datasets, (F) Cell segmentation performance measured by Dice score in Bx1 dataset using cell-interior mask segmentation alone (blue), optical flow alone (orange) and by the proposed multi-pronged approach combining optical flow and segmentation results (green). (G) Solidity measure for nuclei and (H) percentage of fenestrated volume in nucleoli in all datasets.

References:

- [1] HM Vergara et al., *Cell* **184**(18) (2021), p. 4819. doi: 10.1016/j.cell.2021.07.017
- [2] A Müller A et al., *Journal of Cell Biology* **220**(2) (2021). doi: 10.1083/jcb.202010039
- [3] L Heinrich et al., *Nature* **599**(7889) (2021), p. 1.
- [4] BD de Senneville et al., *Communications biology* **4**(1) (2021), p. 1. doi: 10.1101/2021.06.15.446847
- [5] W Shen et al., *Proceedings of the IEEE International Conference on Computer Vision* (2017), p. 2391-2400.
- [6] G Farnebäck in “Scandinavian conference on Image analysis”, (Springer, Berlin, Heidelberg), p. 363-370.
- [7] This project was carried out with major support from the OHSU SMMART Program, National Institutes of Health (NIH), National Cancer Institute (NCI) Human Tumor Atlas Network (HTAN) Research Center (U2CCA233280), the Prospect Creek Foundation, OHSU Brenden-Colson Center for Pancreatic Care, a NIH/NCI Cancer Systems Biology Consortium Center (U54CA209988), and the Knight Cancer Institute Cancer Center Support Grant (5P30CA69533). Electron microscopy was performed at the OHSU Multiscale Microscopy Core, an OHSU University Shared Resource.